Strain Response and Performance of Subgrades and Flexible Pavements Under Various Loading Conditions

BRYAN D. PIDWERBESKY

Specific fundamental loading parameters (load magnitude and number of repetitions, tire inflation pressure, and basic tire type) that influence the behavior of thin-surfaced granular pavements were examined. The pavement response and performance measurements included continuous surface deflection basins, longitudinal and transverse profiles, and vertical strains in the granular layers and subgrade. The first pavement trial considered only the elastic response of a thin-surfaced, unbound granular pavement over a weak subgrade, to varying wheel loads, tire inflation pressures, and two basic tire types (bias and radial ply). The axle load had the greatest effect on pavement response and the tire type had no apparent effect, but increases in the tire pressure resulted in slight decreases in the magnitude of the vertical compressive strain in the subgrade and unbound granular cover. Two subsequent pavements were tested to study the relationship between elastic response at different cumulative loadings and the structural capacity of each pavement. The magnitudes of the resilient strains measured are substantially greater than the levels predicted by the models on which current flexible pavement design procedures are based for the same number of loading repetitions to failure. Subgrade strain models for thin-surfaced unbound granular pavements are evaluated. The pavement construction, loading routine, analysis, and results are discussed.

The New Zealand model used for designing the thicknesses of thin-surfaced, unbound granular flexible pavement layers assumes that surface thicknesses of less than 35 mm do not contribute to the structural capacity of the pavement and that the stresses are dissipated through the depth of the granular cover layers above the subgrade. The subgrade strain criterion for flexible pavements in the *Shell Pavement Design Manual* (*1*),

$$\epsilon_{CVS} = 0.028\ N^{-0.25} \quad (1)$$

where ϵ_{cvs} is the vertical compressive strain in the subgrade, and N is the number of repeated equivalent single axle loads, is the basis of the New Zealand subgrade strain criteria for limiting rutting. The subgrade strain criteria for primary and secondary highways, respectively, in New Zealand are (*2*)

$$\epsilon_{CVS} = 0.021\ N^{-0.23} \quad (2)$$

$$\epsilon_{CVS} = 0.025\ N^{-0.23} \quad (3)$$

In New Zealand, the term for equivalent single-axle load is equivalent design axle (EDA). One EDA is defined as one passage of an 80-kN single-axle load on dual tires inflated to 550 kPa. Other axle loads are related to the reference axle by the fourth-power rule (the exponent is 4).

University of Canterbury, Private Bag 4800, Christchurch, New Zealand.

However, the flexible pavement design model is based on multilayer linear elastic theory and assumes that the pavement material properties can be characterized by linear elastic, homogeneous, and isotropic behavior, whereas, in reality, the behavior of unbound granular materials tends to be nonlinear, elastoplastic, nonhomogeneous, and anisotropic. Because of the unique situation in New Zealand, with respect to the road user charges incurred by the road transport industry and the dependence on thin-surfaced flexible pavements, research was needed to verify the subgrade strain criteria. The research described in this paper involved a series of instrumented pavements constructed in the Canterbury Accelerated Pavement Testing Indoor Facility (CAPTIF) and subjected to a variety of tire pressures, tire types, and loads.

DESCRIPTION OF FACILITY AND INSTRUMENTATION

The main feature of CAPTIF is the Simulated Loading and Vehicle Emulator (SLAVE), illustrated in Figure 1; the primary characteristics are summarized in Table 1. SLAVE "vehicles" are equipped with half-axle assemblies that can carry either single or dual tires. The configuration of each vehicle, with respect to suspensions, wheel loads, tire types, and tire numbers, can be identical or different for simultaneous testing of different load characteristics.

Electronic systems have been acquired or developed to measure subsurface strains and temperatures, transverse and longitudinal surface profiles, and pavement rebound. The CAPTIF deflectometer measures the surface rebound of a pavement under the influence of a wheel load to the nearest 0.01 mm every 50 mm of horizontal movement in much the same way as a Benkelman beam except that the former uses an electromagnetic gap-measuring sensor at the end of the beam to measure the vertical distance between the sensor and a target disk placed on the pavement surface. The CAPTIF profilometer measures the transverse surface profiles to an accuracy of ± 1 mm.

The soil strain measuring systems determine extremely small strains with high resolution using Bison soil strain sensors. The gauge length is the separation distance between each paired coil; strain (ϵ) is the quotient of the change in gauge length (ΔL) divided by the initial gauge length (L). The strain disks are installed during the formation of the subgrade and the overlying pavement layers, resulting in negligible disturbance to the materials. The strain disks have a diameter of 50 mm and are 7 mm thick.

Two data-acquisition systems for the Bison strain coils were used. In the interim system, all the coils in an array were connected

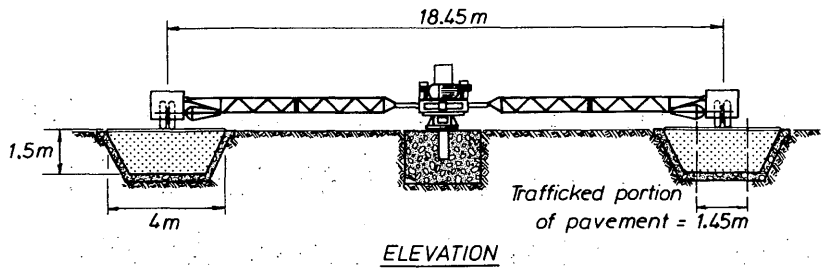

FIGURE 1 SLAVE and cross section of track.

to a manual switching apparatus. Then, the two leads from the switching apparatus were connected to a Bison soil strain gauge, Model 4101A, a single-channel linearizing monitor that supplied the alternating current to the transmitter coil and measured the output from the paired coil. The output voltages from the gauge and pavement temperature probes were recorded through the HP Model 3852S data-acquisition unit using an HP 44711A 24-channel FET multiplexer module. The output from the multiplexer was fed into a 13-bit digital voltmeter (HP 44702A). The data-acquisition unit stored the data in memory before downloading them to an HP PC308 controller board installed in an IBM-compatible AT. The error in the interim strain-measuring system was ±50 μm/m. Before installation, the sensors were calibrated to generate an output voltage versus separation distance relationship for each sensor configuration. During the loading routine, the normal sampling rate was 100 Hz, but the sampling rate increased to at least 10 kHz (depending on the vehicle speed) for a 0.5-sec period whenever triggered by the test vehicle cutting an infrared beam at the start of the instrumented pavement section.

The permanent system is a modified prototype of the more sophisticated Saskatchewan soil strain displacement-measuring (SSSD) system, developed by Saskatchewan (Canada) Highways and Transportation. SSSD is essentially a computer and associated units containing custom-built control, general-purpose input-output, transmitter, and receiver boards. Once triggered by the moving vehicles' cutting a light beam, all the sensors in an array are scanned simultaneously every 30 mm of vehicle travel, and a continuous bowl of strain-displacement versus distance traveled is obtained.

Dynamic wheel forces are dominated by the behavior of sprung mass, so the wheel forces are the sum of the vehicle mass multiplied by the chassis acceleration and the unsprung mass multiplied by the vertical axle acceleration. The dynamic loads were quantified by the vertical acceleration measured by PCB 308B accelerometers mounted on each vehicle. The piezoelectric accelerometers have a linear response from 1 to 3,000 Hz of 100 mV/g. The accelerometers were connected to a PCB 483A 12-channel signal conditioning unit, and the signals were recorded on a Hewlett-Packard 3968A instrumentation recorder. The analog signals were digitized using the HP 3852 data acquisition system sampling at 200 Hz per channel.

FULL-SCALE PAVEMENT INVESTIGATIONS

The experiment involved constructing three sequential test pavements at CAPTIF (Stages 1, 2, and 3). In Stage 1, the pavement response to the primary loading variables (load magnitude, tire inflation pressure, and basic tire type, all on dual-tired wheels) were measured. The final two stages involved testing the life-cycle performance of different pavements and subgrades under selected loading conditions.

Stage 1 Pavement Response to Different Loading Conditions

Initial tasks included selecting and developing instrumentation and data-acquisition systems and preparing the vehicles and track. The silty clay subgrade had a California bearing ratio (CBR) of 5 percent at its natural moisture content. The liquid limit and plasticity index were 43 and 23 percent, respectively. The base course aggre-

TABLE 1 Characteristics of SLAVE

Item	Characteristic
Test Wheels	Dual- or single-tires; standard or wide-base; bias or radial ply; tube or tubeless; maximum overall tire diameter of 1.06 m
Load of Each Vehicle	21 kN to 60 kN, in 2.75 kN increments
Suspension	Air bag; multi-leaf steel spring; single or double parabolic
Power drive to wheel	Controlled variable hydraulic power to axle; bi-directional
Transverse movement of wheels	1.0 m centre-to-centre; programmable for any distribution of wheelpaths
Speed	0-50 km/h, programmable, accurate to 1 km/h
Radius of Travel	9.1 m

SLAVE is designed to be operated continuously without supervision.

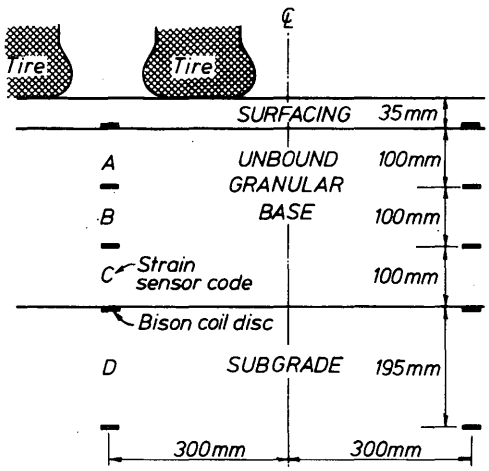

FIGURE 2 Array of strain coil sensors.

gate was a well-graded crushed river gravel (Canterbury greywacke) with a laboratory CBR of 80 percent. The moisture content during compaction was 5 percent. The surfacing was an asphalt concrete consisting of a graded aggregate (maximum particle size 10 mm), 6.4 percent bitumen, and 4.7 percent air voids. The penetration grade of the bitumen was 80/100. The bulk density and bulk specific gravity of the mix were 2 300 kg/m^3 and 2.306, respectively, and the mix temperature was 155°C. The Marshall stability and flow were 18.1 kN and 4.3 mm, respectively.

The bottom layer in the track consisted of a drainage layer of coarse gravel 150 mm thick covered with a nonwoven geotextile. On top of that was an 800-mm-thick layer of well-compacted loess. The bottom coil of each vertical strain sensor array was carefully positioned in the top of the loess. The subgrade layer of silty clay was placed and compacted to a 200-mm depth over the loess. All layers of the subgrade and the granular cover were spread by a small bulldozer and compacted by a Sakai SW41 (40-kN) dual drum roller.

The next set of strain sensors and a set of temperature probes were placed at the interface of the subgrade and granular cover layers. Then, a spunbonded polypropylene geotextile was placed over the subgrade to facilitate the determination of subsurface layer profiles following the testing routine. The granular cover was constructed in three 100-mm lifts, to aid compaction and to allow installation of the paired strain sensors at 100-mm gauge lengths without disturbing the materials. Each array of strain sensors was installed, as shown in Figure 2. Temperature probes were placed at two levels in the granular cover beside the strain coils.

In the uppermost 50 mm of the crushed rock base course, the maximum particle size was only 20 mm to aid workability and compaction. The surface of the base was finished with a pneumatic-tired roller, then a tack coat of emulsified bitumen (60 percent, 180/200 penetration grade) was sprayed. The asphalt concrete was placed, leveled by hand, and compacted. A 3-m straight-edge beam was used to check the roughness, and the maximum deviation was 4 mm. The thickness of the nonstructural surfacing was 35 mm (± 3 mm), which was too thin for inclusion of any instrumentation.

The dynamic characteristics of each vehicle were evaluated to confirm that they were similar. Dynamic wheel forces were measured at a constant speed of 40 km/hr. The vehicles exhibited similar dynamic characteristics, as shown in Table 2.

Vehicle A carried a constant half-axle load of 40 kN (equating to a full axle load of 80 kN) with dual bias ply tires inflated to 550 kPa, so that it was a reference throughout the testing routine. The characteristics of Vehicle B were modified. The maximum cold tire inflation pressures allowed by the tire supplier were 700 and 825 kPa for the bias and radial ply, respectively. All radial and bias ply tires were 10.00R20 and 10.00×20, respectively. The experimental matrix of loading conditions of Vehicle B is shown in Table 3.

The surface deflection bowls, and the vertical strains at various depths in the pavement and subgrade were measured for each of the 20 loading conditions. The strains were measured under the center of the dual tires. Longitudinal and transverse profiles were measured after specified increments of cumulative loading cycles. After the experimental matrix was completed, the maximum surface rut depth was only 7 mm; the deformation within the unbound granular pavement was 2 to 3 mm, which was insufficient to have affected the properties of the pavement.

Deflection basins were measured at three locations on the test section and averaged to determine one basin for each experimental point. The deflection basins were compared on the basis of (a) tire type, (b) tire inflation pressure, and (c) wheel load; neither tire type nor tire inflation pressure had a substantial effect on the deflection basin shape. In general, the peak deflection value was independent of tire type. Also, tire pressure had a negligible effect on the peak deflection. The major influence on peak deflection was the wheel load.

The vertical compressive strains were measured in three layers (upper base course, lower base, and subgrade) for each of the 20 loading conditions. The peak compressive strains are defined as the difference between the nominal average residual strain recorded before the approach of the test vehicle to the sensor and the maximum strain (averaged over five cycles) measured under the test vehicle. Figure 3 (*top*) shows a representative sample of the original data from the subgrade, for one specific loading condition (dual radial tires, inflated to 825 kPa and loaded to 40 kN). The longest

TABLE 2 Dynamic Load Coefficients (dlc)

Vehicle	Wheel Load (kN)	Tire Pressure (kPa)	Tire Type	dlc
A	40	580	Bias ply	0.22-0.24
B	40	580	Radial ply	0.22-0.24
B	46	825	Radial ply	0.16-0.18

$$\text{Dynamic load co-efficient (dlc)} = \frac{\text{Standard Deviation of Wheel Forces}}{\text{Static Load}}$$

TABLE 3 Sequence of Loading Conditions on Vehicle B

Bias ply Tires			Radial ply Tires		
Test No.	Pressure (kPa)	Wheel Load (kN)	Test No.	Pressure (kPa)	Wheel Load (kN)
1	550	40	9	825	46
2	700	40	10	700	46
3	700	21	11	550	46
4	550	21	12	550	31
5	550	31	13	825	31
6	700	31	14	700	31
7	700	46	15	700	21
8	550	46	16	550	21
			17	825	21
			18	825	40
			19	700	40
			20	550	40

spikes represent the passage of a wheel load directly over the sensors, and the lessor spike is the passage of the reference wheel load (dual bias ply type inflated to 550 kPa and loaded to 40 kN) at a transverse distance of 0.6 m. For every loading condition and strain measurement in the subgrade, some vertical compression remained after the passage of each wheel load. Then, when the other wheel load passed over the station, the compression disappeared and the subgrade reverted to the original situation. This phenomenon was repeated for all loading cycles.

If it was simply a case of the paired coil disks becoming misaligned, the effect would have increased with cumulative cycles; but this did not occur. Instead, the subgrade was compressed when one wheel load passed directly over the sensor, then shear forces created by the other wheel load traveling in a wheel path 0.6 m away laterally resulted in extension in the layer, and the sensor returned to its original position. Similarly, in the base course, the residual compression induced by one vehicle passing directly over the sensors was eliminated by extension as the other vehicle passed over a point 0.6 m away transversely, but there was no discernible resilient compression as the second vehicle passed over, as shown in Figure 3 (*bottom*). This cyclic compression and extension contributed little to the permanent deformation of the layers, which is the primary criterion for the model describing the performance of thin-surfaced unbound granular pavements, but could affect the degradation of the materials.

The magnitude of the vertical compressive strain in the subgrade and the base course (Figure 4) decreased slightly as the tire inflation pressure increased, for every wheel load. The vertical compressive strain in the granular layers and the subgrade must be dependent upon the zone of influence of the load as well as the contact area and speed of the vehicle. Thus, when the speed is constant and the contact area is reduced, at higher tire inflation pressures, the zone of influence of the load in the pavement and subgrade is reduced, thereby reducing the strain induced in the subgrade in the same manner as strain magnitude reduces under increasing vehicle speed.

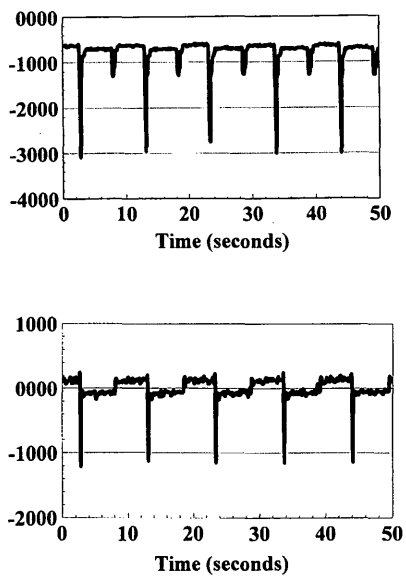

FIGURE 3 Vertical compressive strain (10E = 06) in subgrade (*top*) and base course (*bottom*) under dual radial-ply tires, 825 kPa cold tire pressure, and 40 kN wheel load.

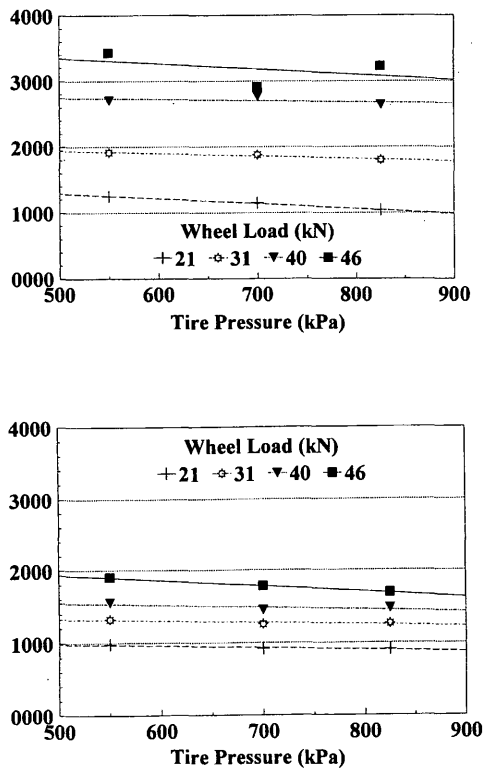

FIGURE 4 Vertical compressive strain (10E = 06) in subgrade (*top*) and base course (*bottom*) under a dual-tired wheel.

Relating Pavement Response to Performance

The objectives of Stages 2 and 3 were to use the system developed in Stage 1 to relate axle loads directly to pavement responses for predicting pavement performance.

Stage 2. Performance of Unbound Granular Base Course Under Thick Asphalt Surface

The Stage 2 pavement had an asphalt concrete surface 85 mm thick (which is thick by New Zealand standards), over a 200-mm unbound granular base course over a clayey subgrade. The in situ CBR of the subgrade for the test section was 13 percent; the subgrade was constructed to achieve a higher bearing capacity (than the Stage 1 subgrade) to achieve a longer pavement life. The base course aggregate was a well-graded crushed river gravel compacted with a moisture content of 4 percent to a maximum dry density of 2 150 kg/m^3. The asphaltic binder was a plastomer-modified bitumen called Practiplast, with a penetration grade of 50 (at 25°C), a softening point of 59.4°C, a viscosity of 2 P (at 169°C), and a shear susceptibility of −0.089 (*3*).

The wheel load was 40 kN for both vehicles for the first 920,000 loading cycles and 46 kN for the remaining 1.2 million loading cycles. The dual radial tires in both vehicles were inflated to 700 kPa. The vehicle speed was 40 km/hr for routine loading and 20 km/hr for the approximately 500 cycles required for completing the strain measurements. The vertical compressive elastic strains in the unbound granular base course and clayey subgrade were measured using arrays of Bison strain coil gauges installed in the subgrade and base course. Altogether, SLAVE applied over 3.2 × 10^6 EDA to the test pavement.

The rut depth at the surface of the test section was only 2 to 4 mm, indicating negligible deformation in the subsurface layers. Surface cracking was insignificant. The project concluded before the predefined failure criterion of a maximum surface rut depth of 25 mm occurred because the maximum allowable overexpenditure on the project was reached (substantial additional research funds were provided) and the next project in the facility had to commence. Stage 2 was conducted simultaneously with another project in the track investigating the effect of different modified binders on the performance of asphalt concrete surface layers, which is reported elsewhere (*3*). It was concluded that the design procedure used was conservative because pavements designed for 1 × 10^6 EDA should have exhibited greater deterioration after 3.2 × 10^6 EDA (*3*). However, according to the New Zealand pavement design procedure (*2*), the pavement had an expected design life of at least 5 × 10^6 EDA.

In the base course, the magnitude of the peak vertical compressive strain decreased slightly during the cumulative loading, from 300 to 220 μm/m. The relationship between the magnitude of the vertical compressive subgrade strain and cumulative loading is shown in Figure 5. The temperatures are the averaged output of the three temperature probes installed directly above the strain sensors in the 85-mm-thick asphalt concrete. Increasing the wheel load from 40 to 46 kN, after 920,000 EDA, resulted in a negligible change in the magnitude of the vertical compressive strain responses in the subgrade (from 1 200 to 1 250 μm/m) and no change in the base course strain. In Stage 1 of this research program, the same increase in wheel load produced a 10 percent increase in the magnitude of the vertical compressive strain in a weak subgrade (CBR of 4 percent under a thin-surfaced, 300-mm unbound granular pavement).

The nominal magnitude of the vertical compressive strain in the subgrade varied between 900 and 1 400 μm/m, and the pavement survived 3.2 × 10^6 EDA without incurring any substantial permanent deformation in the pavement or subgrade. When the temperature of the asphalt concrete decreased thereby increasing the asphalt modulus, the subgrade strain decreased because the stiffer asphalt is more effective in dissipating the stresses from the wheel load.

The AUSTROADS (Australian) subgrade strain criterion (*4*), converted to the same format as Equation 1, is

$$\epsilon_{CVS} = 0.0085\, N^{-0.14} \quad (4)$$

Using Equations 1, 2, and 4, the maximum allowable vertical compressive strain in the subgrade would have been 660, 670, and 1045 μm/m, respectively, for that number of loading cycles, assuming that the pavement would have failed at that point. The Shell and New Zealand subgrade strain criteria (Equations 1 and 2, respectively) are definitely conservative, but the AUSTROADS criterion permits higher strains, which are within the range of the actual strain values measured in this case. Also, the lack of adverse environmental effects would have contributed to extending the life of the pavement.

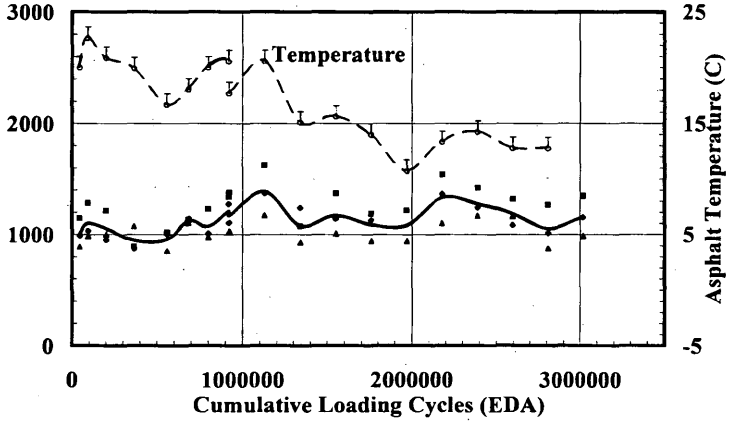

FIGURE 5 Vertical compressive strain (10E = 06) in subgrade under Stage 2 pavement (temperature measured at mid-depth of asphalt layer).

Stage 3. Life-Cycle Performance of Thin-Surfaced Unbound Granular Pavement

The test pavement for this trial consisted of a 25-mm asphalt concrete surfacing layer over 135-mm-thick base course of unbound granular aggregate on a silty clay subgrade of CBR 13 percent; the material properties are the same as those described. The pavement responses and properties were measured as previously described. The pavement was subjected to a constant loading condition (40-kN load and dual radial tires inflated to 825 kPa) until the loading concluded at 740,000 EDA, when the permanent vertical deformation (rut depth) of the surface reached 28 mm (the definition of failure was a maximum rut depth of 25 mm).

The maximum rut depths over the whole pavement were in the range of 15 to 28 mm. In the excavated trenches, the asphalt concrete surfacing and base course of unbound aggregate compacted 8 and 7 mm, respectively, at the centerline under the cumulative loading. The permanent deformation in the subgrade varied between 1 and 13 mm. Most (75 percent) of the permanent deformation occurred in the first 100,000 EDA, then the rutting progressed at a relatively constant rate of 9 μm per loading cycle (one loading cycle equals one EDA). The only significant difference in the longitudinal surface profiles before loading commenced and at the end of the trials was where a localized failure was repaired.

The peak surface deflection was approximately 1.6 mm throughout the life of the pavement, except for a temporary 0.15-mm increase in surface deflection that occurred between 100,000 and 200,000 cumulative EDA. The deflection bowl shapes were the same temporally as well, indicating that the relative moduli of the various layers did not change.

Figure 6 (*top*) illustrates how, after the initial sharp increase in magnitude in the peak vertical compressive strain in the subgrade (ϵ_{cvs}), the strain under cumulative loading varied little, except for the significant decrease at 220,000 EDA. The magnitude of the peak vertical compressive strain in the base course slowly decreased during the first 300,000 loading cycles, from 3 200 to 2 350 μm/m, then remained relatively constant, as shown in Figure 6 (*bottom*).

Until approximately 300,000 EDA, surface deflections and vertical compressive strain levels in the base course and subgrade layers fluctuated. The base course strain levels tended to decrease in magnitude. The magnitude of the subgrade strain tended to increase, until the pavement and subgrade responses achieved a stable condition, with only minor fluctuations in the response to load.

Using Equations 2 and 4, the maximum allowable vertical compressive strains in the subgrade for 740,000 EDA are 940 and 1 280 μm/m, respectively, which are substantially less than the actual strains of approximately 2 800 μm/m. Table 4 shows that the actual strains are two to three times the theoretical maximum strain magnitude allowed by the different criteria, which suggests that the criteria on which the pavement thickness design charts are based could be conservative. However, as before, the strain permitted by the AUSTROAD subgrade criterion (Equation 4) for 740,000 EDA is closer to the measured strains, as shown in Figure 7.

Similar results from a field study involving a privately owned sealed forestry road on the North Island of New Zealand were reported (*5*). In the field study, an instrumented thin-surfaced unbound granular pavement carried logging trucks with axle loads varying from 80 to 160 kN per axle. The strain responses were measured using Bison strain sensors installed in the base course and subgrade. It was found that the strains induced in the subgrade were as much as four times the strains allowed by the subgrade strain criterion, but the pavement performance was acceptable (*5*).

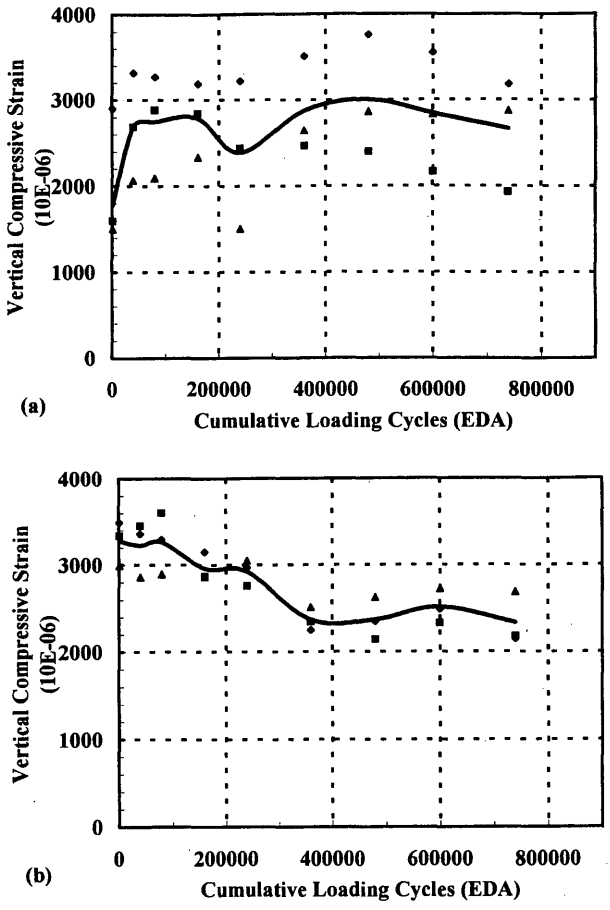

FIGURE 6 Vertical compressive strain (10E = 06) in subgrade (*top*) and base course (*bottom*) under Stage 3 pavement.

CONCLUSION

CAPTIF was used to investigate the fundamental behavior of subgrades and unbound granular pavements under various loading conditions. An electronic-based data-acquisition system for accurately measuring strains in unbound granular layers and subgrades has been developed and used successfully in a number of projects. Instead of relying on simplistic relationships between static axle loads and performance, fundamental pavement responses can be measured for input to pavement performance prediction models. Any procedures for determining load equivalency factors must also consider the type of pavement and the bearing capacity of the subgrade.

With respect to pavement and subgrade response to loading and for the specific conditions of the investigation, the tire type (10.00R20 radial and 10.00×20 bias ply) had an insignificant effect, and the tire inflation pressure (between 550 and 825 kPa) had a minor effect. The vertical compressive strain in the subgrade and unbound granular layers of the pavement decreased slightly as the tire pressure increased.

The magnitude of the vertical compressive strain in the subgrade increased initially, then remained relatively constant. The vertical

TABLE 4 Allowable Vertical Compressive Strain Models Compared with Actual Values

Pavement Number	Number of Load Repetitions (EDA)	Maximum Allowable Vertical Compressive Strain (μm/m) in the Subgrade:				
			New Zealand			Actual (Nominal Value)
		Shell[a]	Primary[b]	Secondary[c]	Australian[d]	
1[e]	3200000	660	670	800	1045	1200
2[f]	740000	955	940	1115	1280	2800

[a] Equation (1)
[b] Equation (2)
[c] Equation (3)
[d] Equation (4)
[e] 85 mm asphalt surface, 200 mm unbound granular basecourse, silty clay subgrade CBR 13%
[f] 25 mm asphalt surface, 135 mm unbound granular basecourse, silty clay subgrade CBR 10%

compressive strain in the unbound base course aggregate tended to decrease slightly in magnitude under cumulative loading; the base course aggregate compacted under repetitive loading and reached a stable condition. The relationship between vertical compressive strains and the cumulative loadings became stable after the pavement was compacted under initial trafficking (in the absence of adverse environmental effects).

The strain magnitudes measured are greater than the levels permitted by the four subgrade strain criteria evaluated; the criteria are intended to govern the allowable vertical compressive strain in the subgrade, to ultimately limit pavement rutting. The subgrade strain criteria are conservative, but the AUSTROADS criteria were the closest to the actual results.

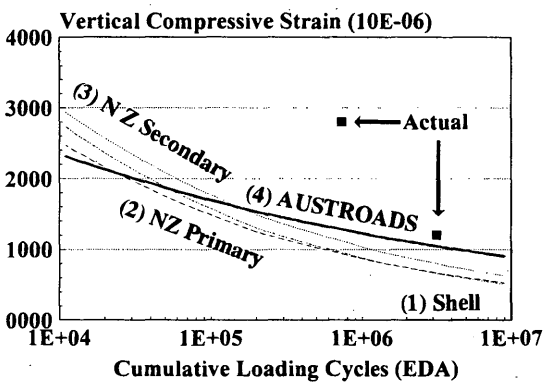

FIGURE 7 Comparison of four subgrade strain criteria governing rutting in flexible pavements.

ACKNOWLEDGMENTS

The author acknowledges the financial support of Transit New Zealand and the University of Canterbury in sponsoring this research project. The author is grateful to A. W. Fussell and G. Crombie for their assistance and to J. de Pont of Industrial Research Limited, Auckland, for analyzing the vertical acceleration data from the SLAVE vehicles. The tires were supplied by Firestone Tires New Zealand Ltd.

REFERENCES

1. *Shell Pavement Design Manual.* Shell International Petroleum, London, England, 1978.
2. *State Highway Pavement Design and Rehabilitation Manual.* National Roads Board, Wellington, New Zealand, 1989.
3. Stock, A. F., L. Planque, and B. Gundersen. Field and Laboratory Evaluation of Specialist High Performance Binders. *Proc., 7th International Conference on Asphalt Pavements,* Vol. 2, Nottingham, England, 1992, pp. 323–337.
4. *Pavement Design—A Guide to the Structural Design of Road Pavements.* AUSTROADS, Sydney, Australia, 1992.
5. Steven, B. D. *The Response of an Unbound Granular Flexible Pavement to Loading by Super-Heavy Vehicles.* Master's thesis. University of Canterbury, Christchurch, New Zealand, 1993.

Publication of this paper sponsored by Committee on Flexible Pavement Design.